7

Modeling physical ageing in polymer composites

H. H U, National Pingtung University of Science and Technology, Taiwan

7.1 Introduction

Physical ageing is a phenomenon displayed as changes in physical and mechanical properties of polymers over time. Above its glass transition temperature (T_g), a polymer can reach thermodynamic equilibrium instantaneously; below T_g, the polymer requires a very long time to achieve thermodynamic equilibrium. During this evolution time, the material properties (i.e. creep rate, stiffness, and strength) change continuously. This gradual process to establish the equilibrium state is known as physical ageing. Physical ageing is not evident over short time periods, but it continues indefinitely over the service life of the polymer or polymer composites. It is therefore essential to understand and be able to model physical ageing in order to assess the long-term durability of polymer composites.

Struik (1978) was the first to conduct a series of systematic creep tests on various polymers to characterize their ageing behaviors. Some of the remarkable conclusions drawn were: (a) physical ageing is a basic feature and is found in all polymers whether polymeric, monomeric, organic, or inorganic; (b) the mechanical properties of glassy polymers strongly depend on the ageing time; (c) in all glassy materials, physical ageing proceeds in a very similar way – during the ageing process, the time-dependent behavior of the glassy material is found to be independent of the specific chemical structure of the material; (d) physical ageing is thermoreversible – this means that when the temperature is above the T_g, physical ageing in a polymer can be erased, below the T_g, physical ageing in polymer starts and can persist for several years. Struik's conclusions are very important for the modeling of physical ageing in polymers and polymer composites.

In Struik's approach, the polymer is first heated to a temperature above the T_g for several minutes and then quenched to a test temperature below the T_g. This process is called rejuvenation. Since physical ageing is thermoreversible, it can be erased from the material by rejuvenation.

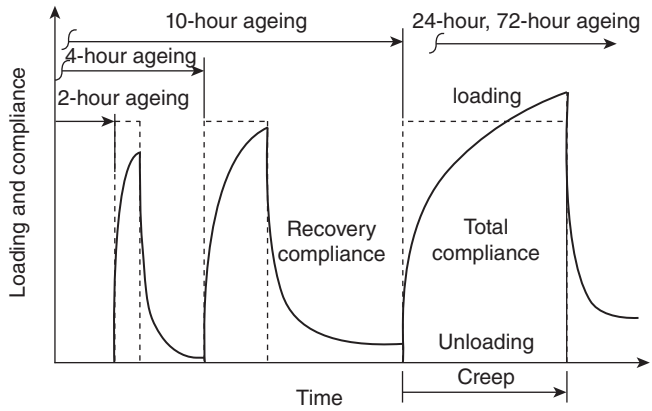

7.1 Momentary creep test process.

After rejuvenation, the temperature remains constant and physical ageing in the material initiates throughout the test. At the end of a certain ageing cycle, a momentary creep test is performed. Figure 7.1 shows the processes involved in a momentary creep test. Momentary creep tests are conducted on the material after 2, 4, 10, 24, and 72 hours of initial ageing cycles. The momentary creep test is defined for a time of less than one-tenth of the initial ageing time. (Struik, 1978). For instance, the creep test time should be less than 0.2 hours following a 2-hour initial ageing. During the momentary creep, the ageing effect on the individual creep compliances is not significant and is negligible so that the material properties can be regarded as constant. However, creep compliances obtained from tests with different initial ageing times are significantly different from one another. Consequently, physical ageing in polymer can be characterized by establishing ageing-related material constants for each momentary compliance curve. Struik's approach has been widely employed to characterize physical ageing in polymer composites. Many experimental works have demonstrated that the ageing behavior of polymer composites is very much like that of polymers.

7.2 Modeling physical ageing in short-term creep

7.2.1 Exponential model

The exponential model is typically employed to characterize physical ageing in polymers and polymer composites. For example, momentary compliances obtained from momentary creep tests can be singled out and plotted on a double logarithmic scale. Figure 7.2 shows the momentary

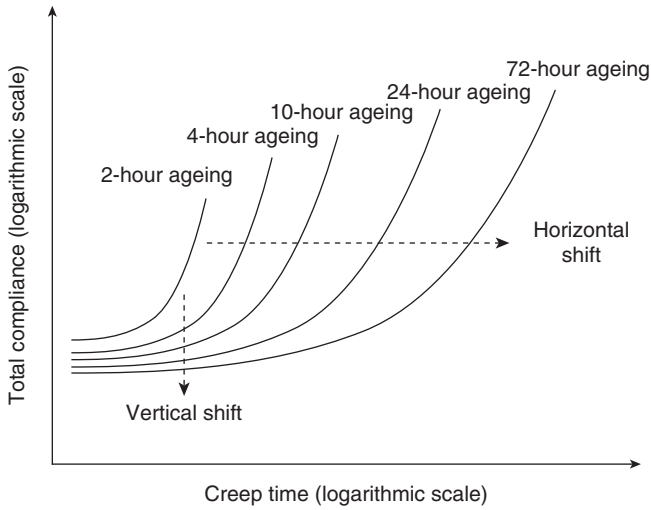

7.2 Exponential model for momentary compliance.

compliances with initial ageing cycles of 2, 4, 10, 24, and 72 hours. The individual momentary compliance can be fitted to an exponential function (Struik, 1978), i.e.

$$S = S_o e^{(t/\tau)^{\beta}} \qquad [7.1]$$

where S_o is initial compliance, t is creep time, τ is relaxation time, and β is a shape factor. It is assumed that the initial compliance and shape factor are constant. Ageing effects can be observed by a horizontal shift of the momentary compliance curves. All momentary compliance curves can be shifted and superposed to a reference curve by introducing a shift factor, i.e.

$$a = \left(\frac{t_{a,ref}}{t_a} \right)^{\mu} \qquad [7.2]$$

where t_a is ageing time, $t_{a,ref}$ is a reference ageing time associated with the reference curve of momentary compliance, and μ is the shift rate which can be obtained from the slope of the test data for shift factor and ageing time, i.e.

$$\mu = \frac{d\log(a)}{d\log(t_a)} \qquad [7.3]$$

Struik (1978) observed that shift rate in all cases is about unity over wide ranges of test temperatures below T_g. When the test temperature is close to T_g, the shift rate significantly decreases to about zero. Moreover, at very

low temperatures, the ageing begins to cease and the shift rate decreases as well. In equation [7.1], relaxation time is considered as the only ageing-dependent parameter, and is given by

$$\tau(t_a) = \tau(t_{a,ref})/a \qquad [7.4]$$

Using shift factor and shift rate, all momentary compliances can be horizontally shifted and superposed to a reference curve, which enables us to fabricate any momentary compliance for any initial ageing time without a creep test.

Struik's model has been generally applied to characterize physical ageing in continuous fiber-reinforced polymer composites. Sullivan (1990) studied physical ageing in glass fiber/thermosetting composites and found that physical ageing significantly affects transverse compliances S_{22} and shear compliance S_{66}, but not S_{11}, S_{12} and S_{21}. In other words, there is no physical ageing in fiber properties and Poisson's ratio. Later, Sullivan and Blais (1993), and Hastie and Morris (1993) obtained similar ageing effects on graphite fiber/thermoset and thermoplastic composites. Brinson and Gates (1995), and Gates and Feldman (1995, 1996) also characterized physical ageing well in transverse, in-plane shear, and quasi-isotropic laminates by using $[90]$, $[\pm45]_s$, and $[0/\pm45/90]_s$ specimens.

Nevertheless, in the horizontal shift of momentary compliance, most of the previous works were unable to achieve an ideal superposition and sometimes a vertical shift is inevitable, as shown in Fig. 7.2. This implies that initial compliance S_o is potentially ageing-dependent. Another challenge is to characterize physical ageing in composites with various fiber orientations. This may result in a large number of creep tests in order to obtain momentary compliances in every fiber orientation.

Hu and Sun (2000b) suggested that elastic and creep compliances can be separated from the total compliance by choosing the data point whose slope is abruptly changed. It was found that creep deformation is very small in comparison with elastic deformation during the initial loading process. Figure 7.3 shows the experimental data for ageing effects on composite AS4/3501-6 with 45° fiber orientation under a test temperature of 148 °C (Hu, 2007). Apparently, elastic compliance decreases to approach a steady-state value as ageing time increases. Momentary creep compliance rate also decreases as ageing time increases. Therefore, physical ageing in elastic and creep compliances can be individually characterized. The experimental data shown in Fig. 7.3(a) can be fitted into an exponential function as

$$S_x^e = S_x^o/(1-\alpha e^{-\gamma t}) \qquad [7.5]$$

where S_x^o is the steady-state elastic compliance in the loading direction; α and γ are constants.

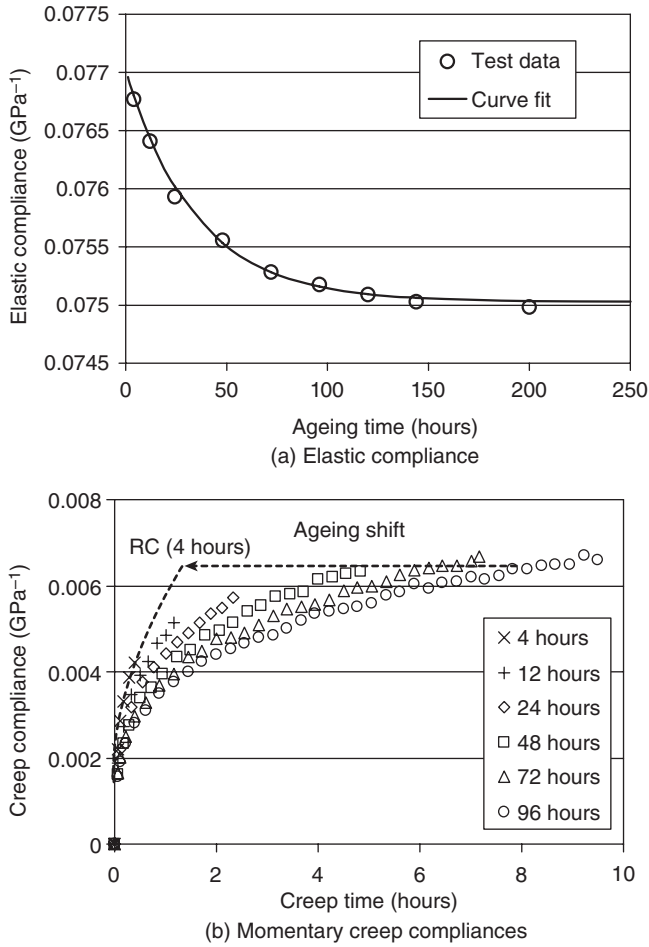

7.3 Physical ageing in composite AS4/3501-6 (45° fiber orientation). RC, reference curve.

7.2.2 Power law model

Creep compliance, as shown in Fig. 7.3(b), can be obtained from the total creep compliance by subtracting elastic compliance. For each initial ageing time, the momentary creep compliance can be fitted into a power law of the form

$$S_x^c(t) = \left(\frac{t}{\tau}\right)^{\beta} \qquad [7.6]$$

where t is creep time, τ is relaxation time, and β is a shape factor. Basically, τ and β are constant for an individual momentary creep compliance curve.

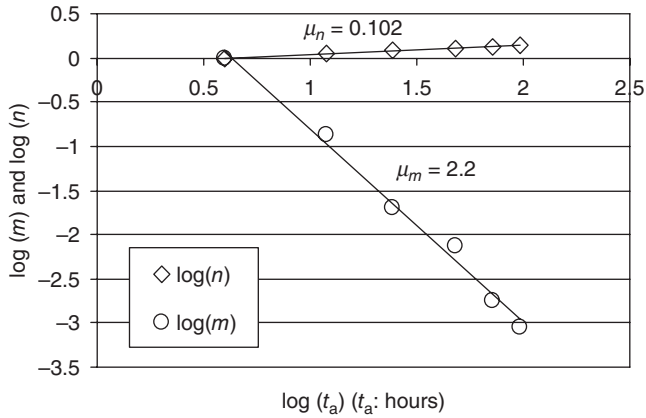

7.4 Shift factors of the momentary creep compliances in Fig. 7.3(b).

For instance, in Fig. 7.3(b), all momentary creep compliances can be shifted and superposed to a reference curve by introducing shift factors, m and n, for relaxation time and shape factor, respectively. The reference curve of momentary creep compliance is given by

$$S^{c}_{x,\mathrm{ref}}(t)=\left(\frac{t}{\tau_{\mathrm{ref}}}\right)^{\beta_{\mathrm{ref}}}=\left(\frac{t}{m\tau}\right)^{n\beta} \qquad [7.7]$$

where $n = \beta_{\mathrm{ref}}/\beta$ and $m = \tau_{\mathrm{ref}}/\tau$. For no loss of generality, the momentary creep compliance curve of 4-hour ageing is taken as a reference curve and the other five curves are shifted and superposed to the reference curve. Five shift factors of m and five shift factors of n are consequently obtained, and they are used to plot logarithmic shift factors versus logarithmic ageing times as shown in Fig. 7.4. In this double logarithmic plot, $\log(m)$ and $\log(n)$ appear to be linear functions of $\log(t_a)$. The slopes, μ_m and μ_n, are obtained from the linear fits, respectively, i.e.

$$\mu_m=-\frac{\mathrm{d}\log(m)}{\mathrm{d}\log(t_a)} \qquad \text{and} \qquad \mu_n=\frac{\mathrm{d}\log(n)}{\mathrm{d}\log(t_a)} \qquad [7.8]$$

where μ_m and μ_n are defined as shift rates. The shift factors m and n can be well fitted in a power law as

$$m=\left(\frac{t_{a,\mathrm{ref}}}{t_a}\right)^{\mu_m} \qquad \text{and} \qquad n=\left(\frac{t_a}{t_{a,\mathrm{ref}}}\right)^{\mu_n} \qquad [7.9]$$

where $t_{a,\mathrm{ref}}$ is reference ageing time corresponding to the reference curve. Consequently, the relaxation time and shape factor of a given ageing time t_a can be related to those of the reference ageing time $t_{a,\mathrm{ref}}$:

$$\tau(t_{\mathrm{a}}) = \tau(t_{\mathrm{a,ref}})\left(\frac{t_{\mathrm{a}}}{t_{\mathrm{a,ref}}}\right)^{\mu_m} \qquad \text{and} \qquad \beta(t_{\mathrm{a}}) = \beta(t_{\mathrm{a,ref}})\left(\frac{t_{\mathrm{a,ref}}}{t_{\mathrm{a}}}\right)^{\mu_n} \qquad [7.10]$$

Theoretically, for the reference curve we should have $m = n = 1$. However, from Fig. 7.4, it is apparent that the reference ageing time that gives the best fit is not the 4-hour ageing. Instead, an ageing time of 4.3 hours with $m = n = 1$ seems to serve better for curve fitting purposes. Using the reference curve, the relaxation time and shape factor for any given ageing time can be fabricated without another momentary creep test.

7.2.3 Effective creep compliance model

The complexity of stress state and creep strain in fiber-reinforced composites leads to the speculation of effective stress and effective creep strain. In general, constant load is applied to the off-axis coupon specimen of composites in creep test. Thus, deformation can be expressed in terms of creep compliance. If off-axis creep compliances can be transformed to effective creep compliances so that all cases can be simply expressed by a single master curve (Hu, 2006).

Parallel to the concept of potential function in plasticity, a potential function f for creep is proposed for a state of plane stress (Chung and Sun, 1993), i.e.

$$2f(\sigma_{ij}) = a_{11}\sigma_{11}^2 + a_{22}\sigma_{22}^2 + 2a_{12}\sigma_{11}\sigma_{22} + 2a_{66}\sigma_{12}^2 \qquad [7.11]$$

where σ_{ij} refer to the principal material directions and the coefficients a_{ij} describe the amount of anisotropy in the initial creep deformation. By using the flow rule, the creep strain increments can be expressed in terms of the creep potential

$$\mathrm{d}\varepsilon_{ij}^{\mathrm{c}} = \frac{\partial f}{\partial \sigma_{ij}}\mathrm{d}\lambda \qquad [7.12]$$

where $\mathrm{d}\lambda$ is a positive scale factor of proportionality. The increment of creep work is given by

$$\mathrm{d}W^{\mathrm{c}} = \sigma_{ij}\mathrm{d}\varepsilon_{ij}^{\mathrm{c}} = 2f\mathrm{d}\lambda \qquad [7.13]$$

Effective stress is defined as

$$\bar{\sigma} = \sqrt{3f} \qquad [7.14]$$

Effective strain increment $\mathrm{d}\bar{\varepsilon}^{\mathrm{c}}$ is defined as

$$\mathrm{d}W^{\mathrm{c}} = \sigma_{ij}\mathrm{d}\varepsilon_{ij}^{\mathrm{c}} = \bar{\sigma}\mathrm{d}\bar{\varepsilon}^{\mathrm{c}} \qquad [7.15]$$

Substitution of equations [7.13] and [7.14] into equation [7.15] yields

$$\mathrm{d}\lambda = \frac{3}{2}\left(\frac{\mathrm{d}\bar{\varepsilon}}{\mathrm{d}\bar{\sigma}}\right)\left(\frac{\mathrm{d}\bar{\sigma}}{\bar{\sigma}}\right) \qquad [7.16]$$

Recalling equations [7.11] and [7.12], we set $a_{22} = 1$ without loss of generality.

Creep strain increment can be expressed as

$$\begin{Bmatrix} \mathrm{d}\varepsilon_{11}^{\mathrm{c}} \\ \mathrm{d}\varepsilon_{22}^{\mathrm{c}} \\ \mathrm{d}\gamma_{12}^{\mathrm{c}} \end{Bmatrix} = \begin{bmatrix} a_{11} & a_{12} & 0 \\ a_{12} & 1 & 0 \\ 0 & 0 & 2a_{66} \end{bmatrix} \begin{Bmatrix} \sigma_{11} \\ \sigma_{22} \\ \sigma_{12} \end{Bmatrix} \mathrm{d}\lambda \qquad [7.17]$$

The coefficients a_{ij} can be determined by uniaxial creep tests of off-axis specimens.

Experiment shows that the creep deformation in the fiber direction is negligible (Hu, 2006). Thus a_{11} and a_{12} are determined to be zero. The creep potential in equation [7.11] is simplified to one parameter function, i.e.

$$2f(\sigma_{ij}) = \sigma_{22}^2 + 2a_{66}\sigma_{12}^2 \qquad [7.18]$$

and equation [7.17] is simplified to

$$\begin{Bmatrix} \mathrm{d}\varepsilon_{11}^{\mathrm{c}} \\ \mathrm{d}\varepsilon_{22}^{\mathrm{c}} \\ \mathrm{d}\gamma_{12}^{\mathrm{c}} \end{Bmatrix} = \begin{Bmatrix} 0 \\ \sigma_{22} \\ 2a_{66}\sigma_{12} \end{Bmatrix} \mathrm{d}\lambda \qquad [7.19]$$

Coefficient a_{66} is the only unknown parameter to be determined. By using coordinate transformation, principal stresses are correlated to the uniaxial stress, i.e.

$$\begin{aligned} \sigma_{22} &= \sigma_x \sin^2(\theta) \\ \sigma_{12} &= -\sigma_x \sin(\theta)\cos(\theta) \end{aligned} \qquad [7.20]$$

where θ is the fiber orientation related to the loading direction x. Substitution of equations [7.20] into [7.14] and [7.18] yields

$$\bar{\sigma} = h(\theta)\sigma_x \qquad [7.21]$$

where $h(\theta) = \sqrt{3/2}\left(\sin^4\theta + 2a_{66}\sin^2\theta\cos^2\theta\right)^{1/2}$. Thus effective stress is related to the applied uniaxial stress σ_x. Substitution of equation [7.21] into [7.14] and [7.15] yields

$$\mathrm{d}\bar{\varepsilon}^{\mathrm{c}} = \frac{\sigma_{ij}\mathrm{d}\varepsilon_{ij}^{\mathrm{c}}}{\bar{\sigma}} = \frac{2}{3}\bar{\sigma}\mathrm{d}\lambda = \frac{2}{3}h(\theta)\sigma_x\mathrm{d}\lambda \qquad [7.22]$$

From coordinate transformation law

$$\mathrm{d}\varepsilon_x^{\mathrm{c}} = \mathrm{d}\varepsilon_{11}^{\mathrm{c}}\cos^2\theta + \mathrm{d}\varepsilon_{22}^{\mathrm{c}}\sin^2\theta - \frac{1}{2}\mathrm{d}\gamma_{12}^{\mathrm{c}}\sin 2\theta \qquad [7.23]$$

where $d\varepsilon_x^c$ is the creep strain increment, which can be measured in the loading direction. Substituting equations [7.19] and [7.20] into equation [7.23], we obtain

$$d\varepsilon_x^c = \frac{2}{3}h^2(\theta)\sigma_x d\lambda \qquad [7.24]$$

Comparison of equations [7.22] and [7.24] leads to

$$d\bar{\varepsilon}^c = d\varepsilon_x^c / h(\theta) \qquad [7.25]$$

For monotonic loading, equation [7.25] is integrable. Therefore, the effective creep strain is obtained, i.e.

$$\bar{\varepsilon}^c = \varepsilon_x^c / h(\theta) \qquad [7.26]$$

The axial creep strain ε_x^c can be measured under uniaxial tension creep test. Combining equations [7.21] and [7.26], effective creep compliance can be expressed as

$$\bar{S}^c(t) = \frac{\bar{\varepsilon}^c(t)}{\bar{\sigma}} = \frac{\varepsilon_x^c(t)}{\sigma_x}\frac{1}{h^2(\theta)} = \frac{S_x^c(t)}{h^2(\theta)} \qquad [7.27]$$

Therefore, in a given ageing time, momentary creep compliance $S_x^c(t)$ with respect to fiber orientation θ can be represented by effective creep compliance. Momentary creep compliance $S_x^c(t)$ can be obtained from uniaxial creep test and a_{66} is the only unknown parameter in $h(\theta)$ to be determined by experiment. In order to validate this model, off-axis coupon specimens with 90°, 45°, 30°, and 15° fiber orientations are tested isothermally at 104 °C after 5, 12, 24, 48, 72, and 96 hours initial ageing (Hu, 2006). Figure 7.5 shows the test data of creep compliances after 5 hours ageing. By choosing a_{66} = 0.95, creep compliances are transformed to effective creep compliances and

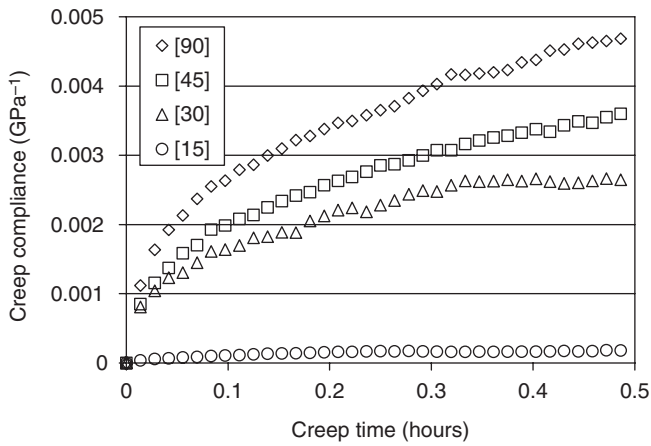

7.5 Momentary creep compliances of 5-hour ageing.

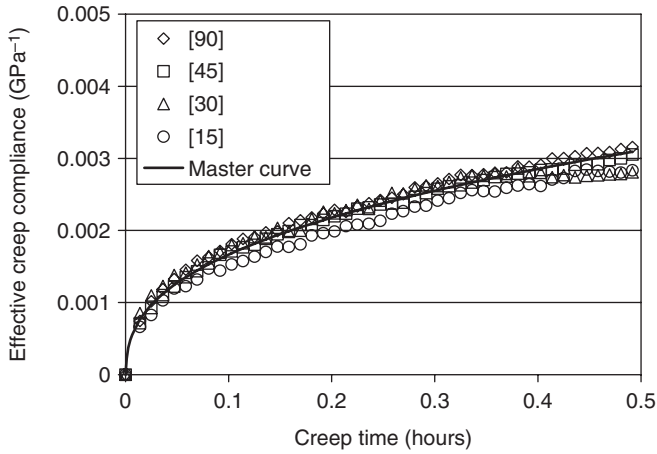

7.6 Effective creep compliances and master curve of 5-hour ageing.

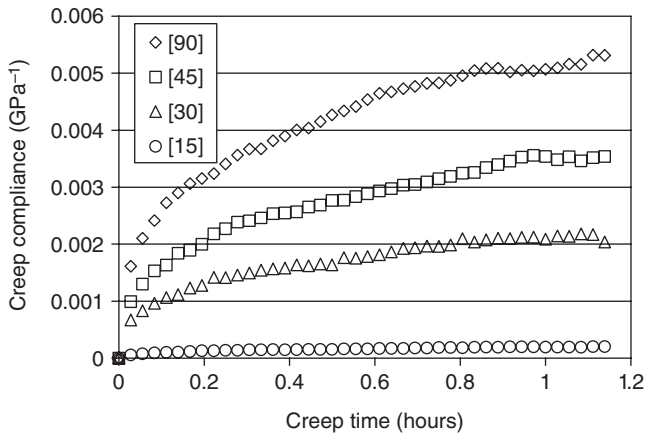

7.7 Momentary creep compliances of 12-hour ageing.

successfully collapsed into a single master curve as shown in Fig. 7.6. The test results obtained from different initial ageing times are shown in Figs 7.7 to 7.16. In all cases, effective creep compliances are successfully collapsed into a single master curve by using the same parameter $a_{66} = 0.95$. As a result, six momentary master curves for different initial ageing times, i.e. 5, 12, 24, 48, 72, and 96 hours, are obtained. Recalling the approach of ageing time shift, the individual momentary master curve can be fitted into a power law function. By introducing shift factors for relaxation time and shape factor, each momentary master curve can be shifted and superposed to a reference

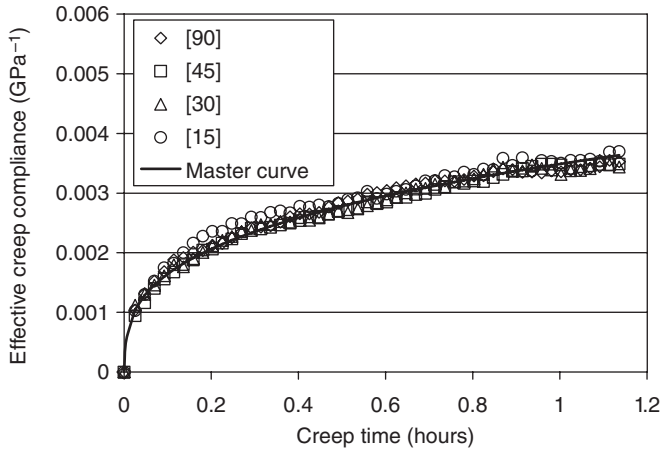

7.8 Effective creep compliances and master curve of 12-hour ageing.

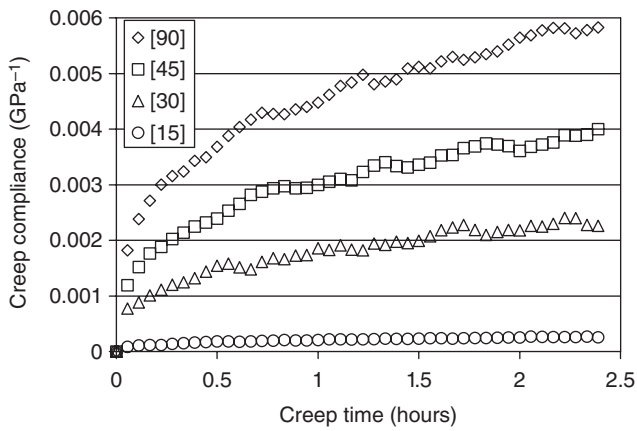

7.9 Momentary creep compliances of 24-hour ageing.

master curve. The shift rates can be obtained from the linear fits of logarithmic shift factor and logarithmic ageing time. Using the reference master curve, the relaxation time and shape factor of a master curve for any given ageing time can be fabricated without another momentary creep test.

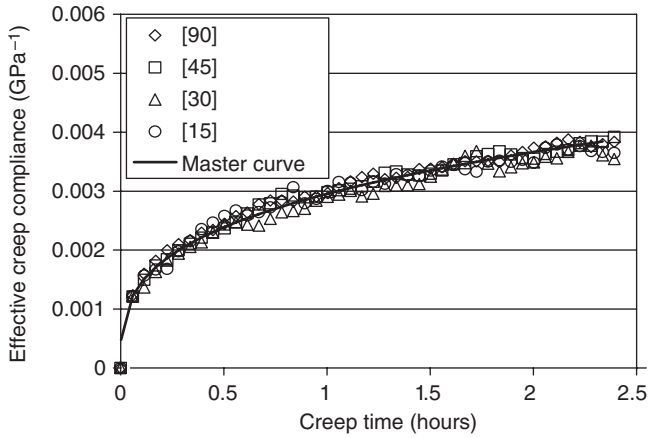

7.10 Effective creep compliances and master curve of 24-hour ageing.

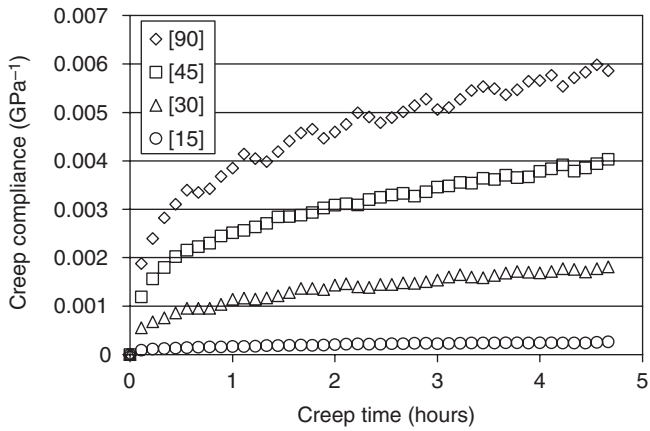

7.11 Momentary creep compliances of 48-hour ageing.

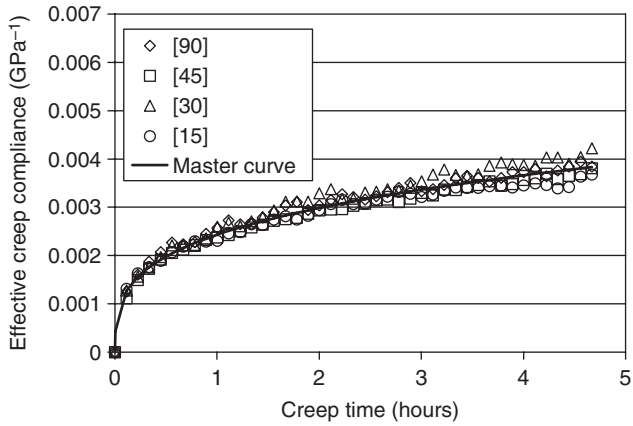

7.12 Effective creep compliances and master curve of 48-hour ageing.

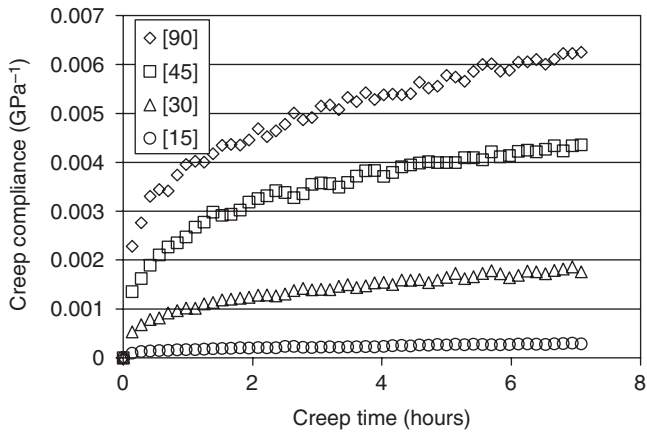

7.13 Momentary creep compliances of 72-hour ageing.

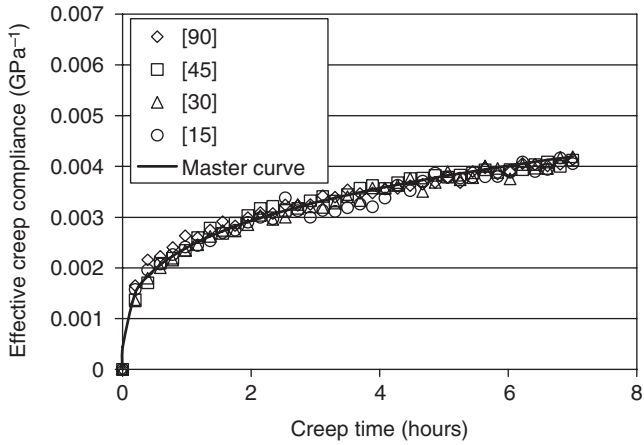

7.14 Effective creep compliances and master curve of 72-hour ageing.

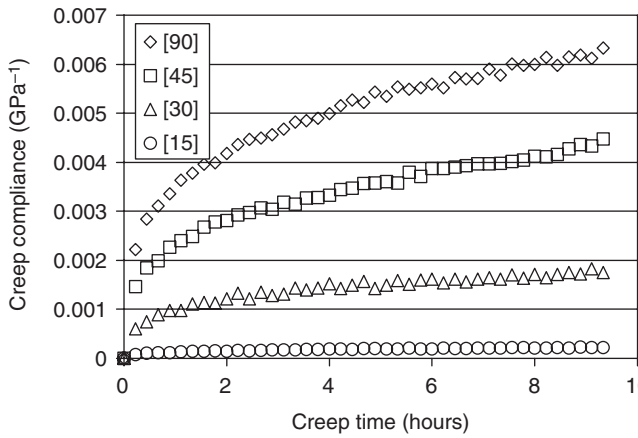

7.15 Momentary creep compliances of 96-hour ageing.

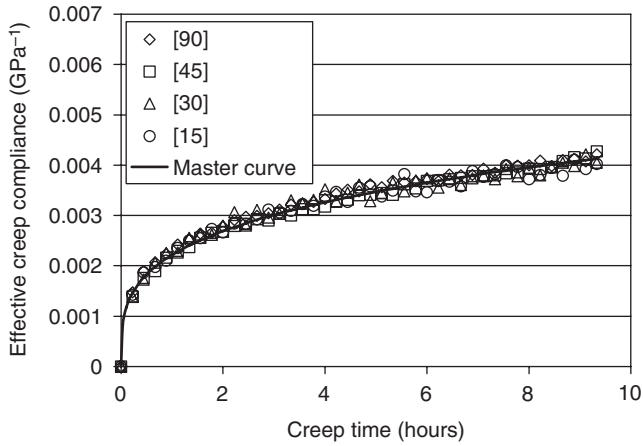

7.16 Effective creep compliances and master curve of 96-hour ageing.

7.3 Modeling physical ageing in long-term creep

7.3.1 Effective time model

It is noted that Boltzmann's superposition principle is based on the assumption that material properties do not change during the mechanical test. This is why the momentary creep test is adopted in the above studies since the ageing effect is not significant and is negligible during the short-time creep test. However, if the creep time is not short in comparison with the previous ageing time, the mechanical properties of polymers continuously change due to physical ageing and therefore Boltzman's superposition principle is no longer valid.

Struik (1978) proposed the concept of 'effective time' to account for the time-dependent nature of the relaxation time and developed a model for the prediction of long-term creep under physical ageing. In his model, a time-dependent shift factor, $a_o(t)$, for relaxation time is introduced to equation [7.1], i.e.

$$S = S_o e^{\left(\frac{t}{\tau_o / a_o(t)}\right)^{\beta_o}} \qquad [7.28]$$

and

$$a_o(t) = \left(\frac{t_a^o}{t_a^o + t}\right)^{\mu} \qquad [7.29]$$

where τ_o is relaxation time associated with previous ageing time, t_a^o, and β_o is shift rate. To compare with equation [7.2], shift factor is no longer a constant but is time-dependent. In the time interval between t and dt, all relax-

ation processes are therefore $1/a$ times slower than at $t = 0$. Thus the interval is equivalent to an effective time interval $d\lambda$ given by

$$d\lambda = \alpha_o(t)dt \qquad [7.30]$$

Based on this equation, the effective time λ can be defined as

$$\lambda = \int_0^t a_o(\xi)d\xi \qquad [7.31]$$

where ξ is an integration parameter on the time scale. Struik defined the effective time model in the form

$$S = S_o e^{(\lambda/\tau_o)^{\beta_o}} \qquad [7.32]$$

Equation [7.32] has been widely adopted to predict the long-term creep of polymer composites under physical ageing.

In the power law model, a master curve for a given initial ageing time t_a^o can be expressed as

$$\bar{S}^c(t) = \left(\frac{t}{\tau_o/m_o}\right)^{\beta o/no} \qquad [7.33]$$

where τ_o and β_o are associated with previous ageing time t_a^o. The shift factors m_o and n_o are ageing time-dependent, i.e.

$$m_o(t) = \left(\frac{t_a^o}{t_a^o + t}\right)^{\mu_m} \quad \text{and} \quad n_o(t) = \left(\frac{t_a^o + t}{t_a^o}\right)^{\mu_n} \qquad [7.34]$$

Equation [7.33] can be expressed in the form

$$\bar{S}^c(t) = \left(\frac{t}{\tau_o/G_o(t)}\right)^{\beta_o} \qquad [7.35]$$

where

$$G_o(t) = \left[m_o(t)\left(\frac{t}{\tau_o}\right)^{(1-n_o(t))}\right]^{(1/n_o(t))} \qquad [7.36]$$

is a time-dependent shift factor for relaxation time. An effective time interval is given by

$$d\lambda = G_o(t)dt \qquad [7.37]$$

Subsequently, the effective time λ is obtained from the integral

$$\lambda = \int_0^t G_o(\xi)d\xi \qquad [7.38]$$

The integration of equation [7.38] can be carried out by numerical methods, therefore the effective time model is obtained

$$\bar{S}^c(t) = \left(\frac{\lambda}{\tau_o}\right)^{\beta_o} \qquad [7.39]$$

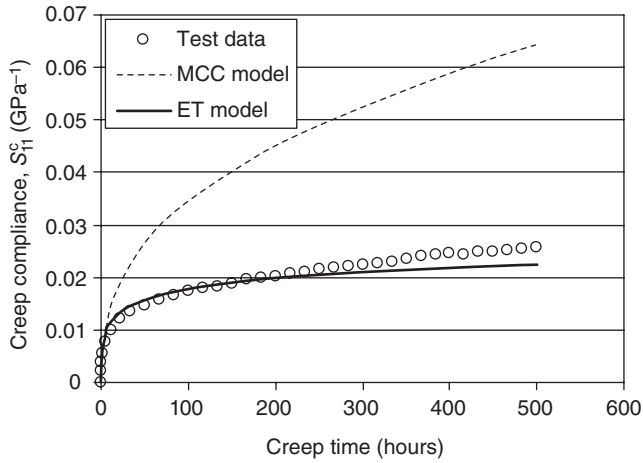

7.17 Long-term creep compliance of 45° off-axis specimen. MCC, momentary creep compliance; ET, effective time.

7.3.2 Long-term creep prediction

The predictions of long-term creep using the power law model have been validated by long-term creep tests (Hu, 2007). After rejuvenation and 5-hour initial ageing, the long-term creep test was conducted on 45° off-axis specimens. Figure 7.17 shows the test result and predictions of long-term creep. During the momentary creep, test data and the predictions of the effective time model and the momentary creep compliance model are almost overlapping. It is again demonstrated that the ageing effect is not significant and is negligible in momentary creep. When creep continues, the prediction of the momentary creep compliance model (dashed line) overestimates the long-term creep. The effective time model (solid line) appears to provide relatively good predictions for long-term creep.

Another validation test was conducted on composite laminate $[90/(+45/-45)_3]_s$ (Hu, 2007). The coupon specimen was initially aged for 5 hours and then subjected to creep test at isothermal 107 °C. Creep time lasted for more than 500 hours. Figure 7.18 demonstrates that the effective time model provides a good prediction for long-term creep after isothermal ageing.

In the exponential model, physical ageing in composite laminate has been characterized by substituting total compliances for elastic compliances in classical laminate theory (Gates and Feldman, 1995, 1996). However, it is necessary to characterize physical ageing in the composite with various fiber orientations in the first place. Heavy experimental workloads are therefore inevitable. Hu (2007) suggested that creep tests can be conducted on the composite laminates directly to obtain the momentary creep compliances

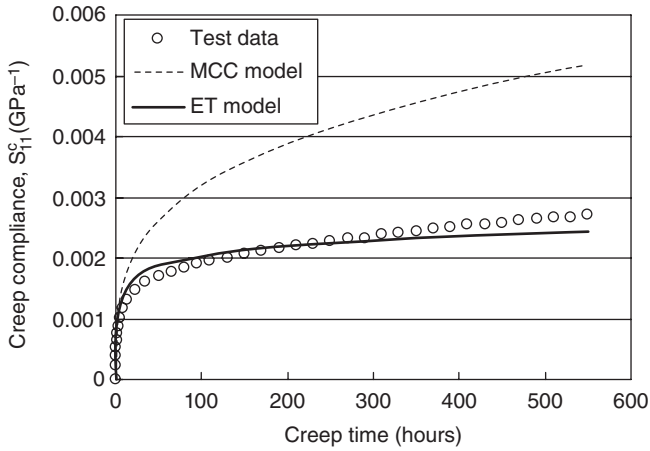

7.18 Long-term creep compliance of laminate $[90/(+45/-45)_3]_s$.

for different ageing times. The power law and effective time models are then employed to predict the long-term creep after physical ageing. This approach avoids the heavy test workload for the composite with various fiber orientations and provides relatively good predictions for long-term creep.

7.4 Temperature and moisture effects

In the course of this study, modeling of physical ageing has been investigated using the isothermal creep test. For cases of non-isothermal creep, an empirical time–temperature/ageing-time shift factor can be expressed (Sullivan, 1990) as

$$\log(a) = \log\left(\alpha t_a^{\mu}\right) + \log(a_T) \qquad [7.40]$$

where α and μ are function of temperature; a_T is function of both temperature and ageing time. This time–temperature shift factor can be experimentally determined and applied to both exponential and power law models.

It has been recognized that the polymeric matrix utilized in reinforced fiber composites absorbs moisture from high-humidity environments. This moisture absorption causes significant changes in the physical and mechanical properties of polymeric composites (Shen and Springer, 1976; Vinson, 1977). In addition, Bueche (1962) found that mixing a polymer with a miscible liquid that contains more free volume than the pure polymer can lower its T_g. Later, Browning *et al.* (1977) also found a depression of T_g in moisture-absorbed 3501-5 neat resin and AS/3501-5 composites using the heat distortion temperature test. DeIasi and Whiteside (1978) and Springer (1982) obtained similar results in neat resins (3501-1, 3501-6, 5208, NMD2373, 3502,

and 934) using thermomechanical analysis. Boil *et al.* (1985) also obtained the same conclusion by testing several composites (AS4/4502, AS4/3501-5A, AS4/3501-6, and AS4/2220-3) with the flexural modulus test.

Hu and Sun (2000a) indicated that the moisture effect is similar to the temperature effect on physical ageing in polymer composites. For instance, for different ageing times, increases in moisture content proportionally relax the elastic compliance of the polymer composite. This behavior resembles that seen with increasing temperature. In addition, the ageing-time shift of creep compliance curves in isothermal creep can be completely applied to the condition of constant moisture content in polymer composites. Hu and Sun (2003) proposed empirical moisture–temperature equivalences to interchange moisture and temperature effects on physical ageing in polymer composites. Such equivalences enable us to replace the complex tests for moisture effects on physical ageing by the tests at the equivalent temperature. Consequently, the modeling of physical ageing developed in isothermal conditions can be applied to model the physical ageing of polymer composites in constant moisture contents.

7.5 Conclusions

Physical ageing is a complex phenomenon that exists in all polymers and the polymer-based matrix of fiber-reinforced composites. Some models have been well developed and, as introduced in this chapter, have characterized ageing effects on stiffness of polymers and polymer composites; however, ageing effects on the strength and damage of polymer composites have not been well studied. Struik (1978) did note that that ageing effects on yielding, charpy impact strength, and environmental stress cracking are not as significant as those on creep compliances; however, whether these conclusions are valid for polymeric composites remains unanswered. In particular, at high stress levels, polymer composites exhibit significant rate-dependent nonlinear stress–strain behavior. Linear viscoelasticity is not able to describe the creep and relaxation behavior of the composite, and nonlinear constitutive models are needed.

7.6 References

BOIL, D. J., BASCOM, W. D. and MOTIEE, B. 'Moisture Absorption by Structural Epoxy-Matrix Carbon-fiber Composites,' *Composites Science and Technology*, **24**, 1985, 253–273.

BRINSON, L. C. and GATES, T. S. 'Effects of Physical Aging on Long Term Creep of Polymers and Polymer Matrix Composites,' *Journal of Solid Structures*, **32** (6/7), 1995, 827–846.

BROWNING, C. E., HUSMAN, G. E. and WHITNEY, J. M. 'Moisture Effects in Epoxy Matrix Composites,' in *Composite Materials: Testing and Design*, ASTM STP 617 (ed. J. G. Davis), ASTM, Philadelphia, PA, 1977, pp. 481–496.

BUECHE, F. *Physical Properties of Polymers*, Interscience Publishers, New York, 1962, pp. 112–118.

CHUNG, I. and SUN, C. T. 'Modelling Creep in Thermoplastic Composites,' *Journal of Composite Materials*, **27**, 1993, 1009–1029.

DEIASI, R. and WHITESIDE, J. B. 'Effect of Moisture on Epoxy Resins and Composite,' in *Advanced Composite Materials – Environmental Effects*, ASTM, STP 658 (ed. J. R. Vinson), ASTM, Philadelphia, PA, 1978, pp. 2–20.

GATES, T. S. and FELDMAN, M. 'Time-dependent Behaviour of a Graphite/Thermoplastic Composite and the Effect of Stress and Physical Aging,' *Journal of Composites Technology and Research*, **17** (1), 1995, 33–42.

GATES, T. S. and FELDMAN, M. 'Effects of physical aging at elevated temperatures on the viscoelastic creep of IM7/K3B,' in *Composites Materials: Testing and Design: Volume*, ASTM STP 1274 (ed. R. B. Deo), ASTM, Philadelphia, PA, 1996, pp. 7–36.

HASTIE, R. L. J. and MORRIS, D. H. 'The Effects of Physical Aging on Creep Response of a Thermoplastic Composites,' in *High Temperature and Environmental Effects on Polymeric Composites*, ASTM STP 1174 (eds C. E. Harris and T. S. Gates), ASTM, Philadelphia, PA, 1993, pp. 163–185.

HU, H. 'Master Curve of Creep in Off-axis Polymeric Composite Laminate,' *Journal of Mechanics*, **22** (3), 2006, 229–234.

HU, H. 'Physical Aging in Long Term Creep of Polymeric Composite Laminates,' *Journal of Mechanics*, **23** (3), 2007, 245–252.

HU, H. and SUN, C. T. 'Moisture Effect on Physical Aging in Polymeric Composites,' *Proceedings of The American Society for Composites*, 2000a, pp. 548–556.

HU, H. and SUN, C. T. 'The Characterization of Physical Aging in Polymeric Composites,' *Composites Science and Technology*, **60**, 2000b, 2693–2698.

HU, H. and SUN, C. T. 'The Equivalence of Moisture and Temperature in Physical Aging of Polymeric Composites,' *Journal of Composites Materials*, **37** (10), 2003, 913–928.

SHEN, C. H. and SPRINGER, G. S. 'Moisture Absorption and Desorption of Composite Materials,' *Journal of Composite Materials*, **10**, 1976, 2–20.

SPRINGER, G. S. 'Moisture Absorption in Fiber-Resin Composites,' in *Developments in Reinforced Plastics* (ed. R. Pritchard), Applied Science Publishers, New York, 1982, pp. 43–65.

STRUIK, L. C. E. *Physical Aging in Amorphous Polymers and Other Materials*, Elsevier Scientific Publishing Company, New York, 1978.

SULLIVAN, J. L. 'Creep and Physical Aging of Composites,' *Composites Science and Technology*, **39**, 1990, 207–232.

SULLIVAN, J. L., BLAIS, E. J. and HOUSTON, D. 'Physical Aging in the Creep Behaviour of Thermosetting and Thermoplastic Composites,' *Composites Science and Technology*, **47**, 1993, 389–403.

VINSON, J. R. (ed.) *Advanced Composite Materials – Environmental Effects*, ASTM STP 658, ASTM, Philadelphia, PA, 1978.